the plant journal

SEB Society for Experimental Biology

*The Plant Journal* (2017) **91,** 1038–1050 doi: 10.1111/tpj.13627

# The $Ca^{2+}$/calmodulin2-binding transcription factor TGA3 elevates *LCD* expression and $H_2S$ production to bolster $Cr^{6+}$ tolerance in Arabidopsis

**Huihui Fang[1], Zhiqiang Liu[1], Yanping Long[2], Yali Liang[1], Zhuping Jin[1], Liping Zhang[1], Danmei Liu[1], Hua Li[3], Jixian Zhai[2,*] and Yanxi Pei[1,*]**

[1]*College of Life Science, Shanxi University, Taiyuan 030006, China,*

[2]*Department of Biology, Southern University of Science and Technology, Shenzhen 518055, China, and*

[3]*College of Environmental and Resource Science, Shanxi University, Taiyuan 030006, China*

Received 15 April 2017; accepted 22 June 2017; published online 3 July 2017.

*For correspondence (e-mails peiyanxi@sxu.edu.cn; zhaijx@sustc.edu.cn).

## SUMMARY

**Heavy metal (HM) contamination on agricultural land not only reduces crop yield but also causes human health concerns. As a plant gasotransmitter, hydrogen sulfide ($H_2S$) can trigger various defense responses and help reduce accumulation of HMs in plants; however, little is known about the regulatory mechanisms of $H_2S$ signaling. Here, we provide evidence to answer the long-standing question about how $H_2S$ production is elevated in the defense of plants against HM stress. During the response of Arabidopsis to chromium ($Cr^{6+}$) stress, the transcription of L-cysteine desulfhydrase (LCD), the key enzyme for $H_2S$ production, was enhanced through a calcium ($Ca^{2+}$)/calmodulin2 (CaM2)-mediated pathway. Biochemistry and molecular biology studies demonstrated that $Ca^{2+}$/CaM2 physically interacts with the bZIP transcription factor TGA3, a member of the 'TGACG'-binding factor family, to enhance binding of TGA3 to the *LCD* promoter and increase *LCD* transcription, which then promotes the generation of $H_2S$. Consistent with the roles of TGA3 and CaM2 in activating *LCD* expression, both *cam2* and *tga3* loss-of-function mutants have reduced LCD abundance and exhibit increased sensitivity to $Cr^{6+}$ stress. Accordingly, this study proposes a regulatory pathway for endogenous $H_2S$ generation, indicating that plants respond to $Cr^{6+}$ stress by adjusting the binding affinity of TGA3 to the *LCD* promoter, which increases *LCD* expression and promotes $H_2S$ production. This suggests that manipulation of the endogenous $H_2S$ level through genetic engineering could improve the tolerance of grains to HM stress and increase agricultural production on soil contaminated with HMs.**

**Keywords: gasotransmitter, hydrogen sulfide, calcium signaling, calmodulin2, transcription factor TGA3, chromium stress.**

## INTRODUCTION

Increased anthropogenic and industrial activities have caused the release of toxic metals into the environment, so contamination of agricultural soil with heavy metals (HMs) has become a serious environmental problem in many developing countries (Wei and Yang, 2010). Chromium (Cr), often present in the forms $Cr^{3+}$ and $Cr^{6+}$, is a serious pollutant of agricultural soil that not only affects crop yield and quality but also causes major concerns for food safety due to its mutagenic and carcinogenic properties (Shanker *et al.*, 2005). There have been reports that plants activate the gasotransmitter hydrogen sulfide ($H_2S$) to defend against HM stress (Zhang *et al.*, 2009; Wang, 2012; Li, 2013; Shi *et al.*, 2014; Jin and Pei, 2015; Fang *et al.*, 2016), but little is known about the regulation of $H_2S$ signaling during the responses of plants to HM stress.

$H_2S$, a multifunctional gasotransmitter, along with nitric oxide (NO) and carbon monoxide (CO), is a topic of interest in organismal studies (Wang, 2002, 2012; Zhang *et al.*, 2011). Research pertaining to endogenous $H_2S$ in higher plants can be traced back to 1978, when $H_2S$ was observed to be released from the leaves of some plants (Wilson *et al.*, 1978). Although emission of endogenous $H_2S$ occurs in higher plants, the positive effects of $H_2S$ have been neglected for many years. Only in the last decade have the physiological functions of $H_2S$ been explored from a new perspective, and this is now an active area of research. $H_2S$

has been found to participate in the regulation of plant development, including seed germination, root morphogenesis, stomatal movement, photosynthesis and flower senescence (Wilson *et al.*, 1978; Pagnussat *et al.*, 2004; Zhang *et al.*, 2011; Jia *et al.*, 2014; Honda, 2015; Papanatsiou *et al.*, 2015; Wang *et al.*, 2016). $H_2S$ is also an important messenger in the adaptation of plants to various abiotic stresses, such as drought, salinity, extreme temperatures, non-ionic osmotic stress and HMs (Wang, 2012; Christou *et al.*, 2013; Li, 2013; Shi *et al.*, 2013; Chen *et al.*, 2015; Jin and Pei, 2015).

In plants, various physiological signals and environmental stimuli can activate $H_2S$ emissions, and $H_2S$ metabolic enzymes have been discovered (Wang, 2012; Jin and Pei, 2015). The cysteine desulfhydrases (CDes) are responsible for the majority of endogenous $H_2S$ production in plants (Rennenberg *et al.*, 1987; Riemenschneider, 2006; Papenbrock *et al.*, 2007). L-cysteine desulfhydrase (LCD), the most unambiguous CDes, catalyzes the hydrolysis of L-cysteine to $H_2S$, ammonia and pyruvate at a stoichiometric ratio of 1:1:1, and its function requires pyridoxal 5′-phosphate as a cofactor (Harrington and Smith, 1980; Rennenberg *et al.*, 1987; Papenbrock *et al.*, 2007). A small fraction of $H_2S$ can also be produced by the *O*-acetyl-L-serine (thiol) lyase (OASTL) family of proteins (Heeg, 2008; Alvarez *et al.*, 2009). DES1, which belongs to the OASTL family based on sequence features, was recently reported as a novel cysteine desulfhydrase, showing a much higher affinity for L-cysteine as a substrate to generate $H_2S$ (Heeg, 2008; Romero *et al.*, 2013).

An appropriate level of $H_2S$ can reduce the accumulation of HMs in millet (Tian *et al.*, 2017), revealing that regulation of endogenous $H_2S$ generation is important for increasing agricultural production and reducing the economic losses caused by HM contamination of cultivated soil. In our previous study, $H_2S$ emission induced by $Cr^{6+}$ stress could be modulated by the calcium ($Ca^{2+}$) level (Fang *et al.*, 2014). However, the molecular mechanism of $Ca^{2+}$-induced endogenous $H_2S$ emission has rarely been reported.

$Ca^{2+}$ is a core transducer and regulator in plant development and defense responses (Sanders *et al.*, 2002; Hetherington and Brownlee, 2004). The transient elevation of intracellular $Ca^{2+}$ is perceived by some downstream members, and then the signal is delivered (Kudla *et al.*, 2010; Peiter, 2011). Calmodulin (CaM) is the primary intracellular $Ca^{2+}$ receptor. After being loaded with $Ca^{2+}$, CaM binds to target proteins and modifies their activities. This CaM-mediated signal transduction accounts for an important portion of $Ca^{2+}$ signaling, and is a delicate system involved in plant defense responses. Some environmental factors can stimulate $Ca^{2+}$ to induce CaM to interact with its target transcription factors (TFs) and thus activate or repress the transcription of target genes (Szymanski and Zielinski, 1996; Park *et al.*, 2005; Doherty *et al.*, 2009; Galon *et al.*, 2010). TGA3, a basic leucine zipper (bZIP) TF, belongs to the 'TGACG'-binding factor (TGA) family (Miao *et al.*, 1994; Miao and Lam, 1995) which participates in some biotic and abiotic stress responses in plants (Jakoby *et al.*, 2002). Additionally, the activity of TGA3 can be regulated by CaMs *in vitro* (Szymanski and Zielinski, 1996).

Here, we present the regulatory pathway of endogenous $H_2S$ emission that is mediated by $Ca^{2+}$/CaM2 signaling during the response of Arabidopsis to $Cr^{6+}$ stress, suggesting potential ways to improve $Cr^{6+}$ tolerance and decrease $Cr^{6+}$ accumulation in grains grown on agricultural lands contaminated by $Cr^{6+}$.

## RESULTS

### $Cr^{6+}$ stress inhibited the elongation of primary roots and induced endogenous $H_2S$ production

To examine the responses of Arabidopsis seedlings to $Cr^{6+}$ stress, primary root elongation and the rate of $H_2S$ production in $Cr^{6+}$-stressed Arabidopsis seedlings were analyzed. After 2 weeks' growth on 1/2 Murashige and Skoog (1/2 MS) medium containing $Cr^{6+}$, the elongation of Arabidopsis roots was restrained in a concentration-dependent manner by $Cr^{6+}$ stress (Figure 1a, b). Significant suppression ($P < 0.05$) was found in plants stressed by 180 μmol $L^{-1}$ $Cr^{6+}$, in which root length was inhibited by approximately 50% (Figure 1a, 1b). Thus, 180 μmol $L^{-1}$ $Cr^{6+}$ was chosen for further stress-based tests. Meanwhile, the rate of $H_2S$ production increased as the $Cr^{6+}$ concentration increased from 0 to 300 μmol $L^{-1}$ (Figure 1b), and the endogenous $H_2S$ content increased by 55% in 180 μmol $L^{-1}$ $Cr^{6+}$ stressed seedlings (Figure 1c). Therefore, we concluded that $Cr^{6+}$ toxicity caused inhibition of root growth and that the generation of the gasotransmitter $H_2S$ was activated during the responses of Arabidopsis to this stress.

### $H_2S$ production was elevated by $Cr^{6+}$ stress through increased *LCD* expression

Because endogenous $H_2S$ emission was increased by $Cr^{6+}$ stress, we investigated the transcription and translation of LCD, which is the key enzyme responsible for $H_2S$ production and which catalyzes the hydrolysis of L-cysteine to $H_2S$, ammonia and pyruvate at a stoichiometric ratio of 1:1:1 (Figure 2a). Data showed that $Cr^{6+}$ stress significantly enhanced the expression of *LCD* at both the transcriptional and translational levels (Figure 2b). As previously reported (Jin *et al.*, 2013), weaker *LCD* expression and a lower $H_2S$ content were detected in the *lcd* mutant, a *LCD* weak allele, which contains a T-DNA insertion in the 3′-untranslated region of the *LCD* gene (Figure 2c). Consistent with the reduced $H_2S$ production, *lcd* was more sensitive to $Cr^{6+}$ stress compared with the wild type (WT), and $Cr^{6+}$ stress

 

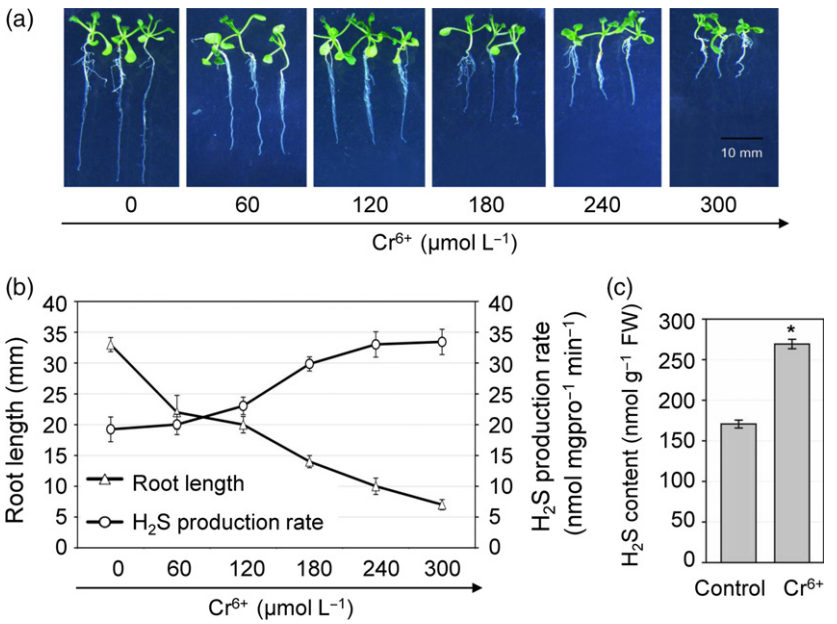


**Figure 1.** $Cr^{6+}$ stress inhibited root elongation and activated endogenous $H_2S$ production in Arabidopsis.
(a) The root phenotype of Arabidopsis seedlings stressed with $Cr^{6+}$.
(b) Root length and endogenous $H_2S$ production rate in $Cr^{6+}$-stressed Arabidopsis.
(c) The endogenous $H_2S$ content in $Cr^{6+}$-stressed Arabidopsis. FW, fresh weight.
The Arabidopsis wild type (Col-0) was grown directly on $Cr^{6+}$ containing 1/2 MS medium (0, 60, 120, 180, 240 and 300 μmol $L^{-1}$ $Cr^{6+}$). Two weeks later, the growth phenotype (a), the primary root lengths and $H_2S$ production rate (b) and the $H_2S$ content (c) were recorded, and the lengths of primary roots were counted from 30 seedlings ($n = 30$). Data are means ± standard error (SE) of three biological repeats, error bars indicate SEs and *indicates a statistical difference ($P < 0.05$). [Colour figure can be viewed at wileyonlinelibrary.com].

caused significant inhibition of root growth in *lcd* seedlings (Figure 2d). In the *lcd* mutant, the activation of $H_2S$ emissions by $Cr^{6+}$ stress was greatly suppressed (Figure 2e). In contrast, when we treated the WT and *lcd* mutant with exogenous $H_2S$, the $H_2S$ content in the *lcd* mutant recovered to the same level as in WT, and exogenous $H_2S$ fumigation further increased the $H_2S$ content in WT and *lcd* under $Cr^{6+}$ stress (Figure 2e). Correspondingly, the toxic symptoms associated with $Cr^{6+}$ stress were alleviated in both the WT and *lcd* mutant upon fumigation with exogenous $H_2S$ (Figure 2f). Thus, $H_2S$ increased the tolerance of Arabidopsis to $Cr^{6+}$ stress and alleviated $Cr^{6+}$ stress-triggered toxic symptoms, which were mediated by the function of LCD in $H_2S$ production.

### $Cr^{6+}$-induced *LCD* expression and $H_2S$ production was modulated by $Ca^{2+}$

The generation of $H_2S$ appeared to be activated in Arabidopsis under conditions of $Cr^{6+}$ stress. Because $Ca^{2+}$ is involved in the $Cr^{6+}$ stress-associated production of $H_2S$ for defense in millet (Fang *et al.*, 2014), to further investigate the function of $Ca^{2+}$ in $H_2S$ production under $Cr^{6+}$ stress we assessed LCD transcription and translation, as well as the $H_2S$ content, with or without $Ca^{2+}$. During $Cr^{6+}$ stress, activation of LCD transcription and translation, as well as the $H_2S$ content, triggered by $Cr^{6+}$ stress increased significantly in the presence of $Ca^{2+}$ but decreased in the presence of the $Ca^{2+}$ chelator ethylene glycol-bis (β-aminoethyl ether)-*N*,*N*,*N*′,*N*′-tetraacetic acid (EGTA) (Figure 3a). Thus, $Ca^{2+}$ may have an important role in $Cr^{6+}$ stress-induced expression of *LCD* and hence in endogenous $H_2S$ production. In the responses of *lcd* to $Cr^{6+}$ stress, the positive effect of $Ca^{2+}$ on $H_2S$ emission was markedly attenuated, and EGTA did not obviously decrease the $H_2S$ content (Figure 3b). Additionally, the knock-down of *LCD* suppressed the positive effect of $Ca^{2+}$, indicating that LCD is a key mediator in $Ca^{2+}$-dependent regulation of $H_2S$ emission during responses to $Cr^{6+}$ stress in Arabidopsis.

We also examined the seedling phenotypes of the $Cr^{6+}$-stressed WT and *lcd* mutant supplemented with $Ca^{2+}$ or $Ca^{2+}$-deprived by EGTA. $Ca^{2+}$ significantly rescued the inhibition of root growth (Figure 3c, d) caused by $Cr^{6+}$ stress in WT seedlings. However, the protective effects of $Ca^{2+}$ were impaired in the $Cr^{6+}$-stressed *lcd* mutant. EGTA aggravated the negative influences of $Cr^{6+}$ on root growth in both WT and *lcd*. In the *lcd* mutant, the combined treatment of EGTA plus $Cr^{6+}$ caused a more dramatic root phenotype and suppressed root elongation (Figure 3c, d).

### The $Ca^{2+}$/CaM2-associated bZIP TF TGA3 specifically binds the 'TGACG' motifs in the *LCD* promoter

As described above, $Ca^{2+}$ is an indispensable mediator in upregulating *LCD* transcription during $Cr^{6+}$ stress. Because of the importance of interactions between *trans*-acting factors and *cis*-acting elements in transcriptional regulation, we hypothesized that $Ca^{2+}$ signaling might trigger *LCD* expression through certain TFs and then activate $H_2S$ synthesis. Signal transduction mediated by CaM occupies a very important position in $Ca^{2+}$ signaling, and our results indicated that $Cr^{6+}$ stress could enhance both the transcriptional and translational levels of CaM2 (Figure 4a). Although the abundance of TGA3 was hardly changed in $Cr^{6+}$-stressed plants (Figure 4a), the promoter region of *LCD* contains core sequences for binding TGA3. Therefore, we speculated that CaM2-mediated $Ca^{2+}$ signaling may modulate the binding activity of TGA3, which regulates

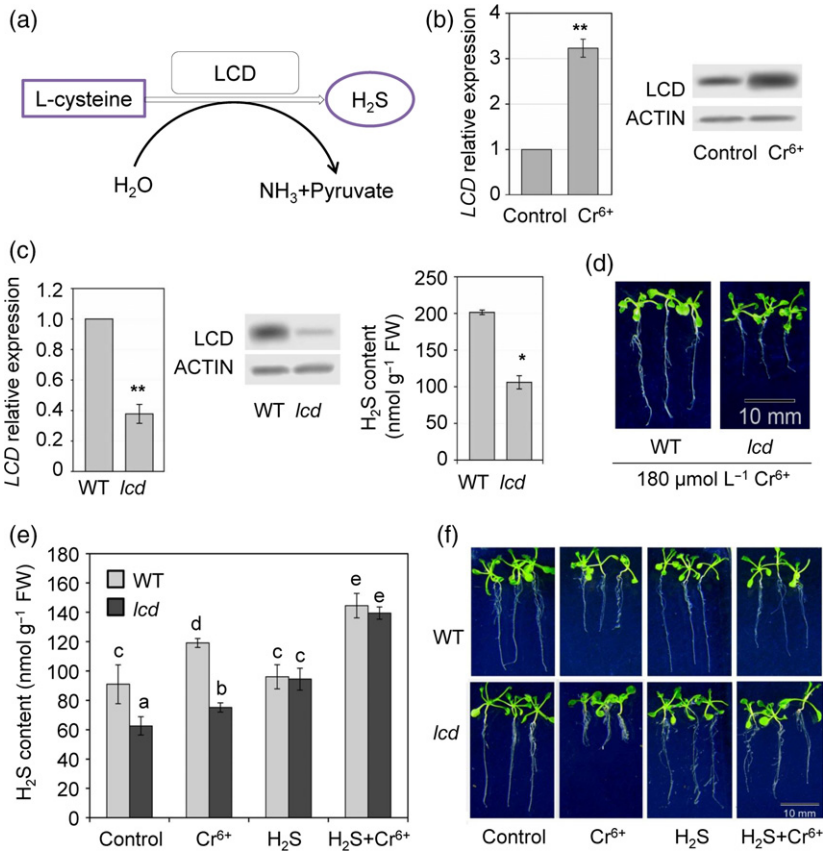


**Figure 2.** $H_2S$ generated by L-cysteine desulfhydrase (LCD) has important functions in defense responses of Arabidopsis to $Cr^{6+}$ stress.
(a). A schematic diagram of $H_2S$ generation mediated by LCD in plants. (b) The transcriptional and translational levels of *LCD* in $Cr^{6+}$-stressed Arabidopsis. The Arabidopsis wild type (WT; Col-0) was grown directly on 1/2 MS medium with ($Cr^{6+}$) or without (CK) 180 μmol $L^{-1}$ $Cr^{6+}$. Two weeks later, *LCD* transcription and translation were detected by real-time quantitative RT-PCR (qRT-PCR) and immunoblotting. (c) *LCD* transcription and translation, as well as $H_2S$ content, in the *LCD* T-DNA insertion mutant *lcd*. The seeds of the WT and *lcd* mutant were grown on 1/2 MS medium. Two weeks later, *LCD* transcription and translation were detected by qRT-PCR and immunoblotting; the $H_2S$ content was detected using a novel polarographic $H_2S$ sensor from 40 WT and *lcd* seedlings. FW, fresh weight. (d) The root growth phenotype of $Cr^{6+}$-stressed WT and *lcd* mutant. The seeds of the WT and *lcd* mutant were grown on 1/2 MS medium containing 180 μmol $L^{-1}$ $Cr^{6+}$. Two weeks later, the growth phenotypes were recorded. (e) The $H_2S$ content in $Cr^{6+}$-stressed WT and *lcd* with exogenous $H_2S$ fumigation. (f) The protective effect of $H_2S$ on root elongation in $Cr^{6+}$-stressed WT and *lcd* plants. The seeds of Arabidopsis WT and *lcd* mutants were grown directly on 1/2 MS medium with or without 180 μmol $L^{-1}$ $Cr^{6+}$, and with or without 50 μmol $L^{-1}$ $H_2S$ fumigation. Two weeks later, the endogenous $H_2S$ contents (e) and the growth phenotypes (f) were recorded from 20 seedlings.
Data are means ± SE of three biological repeats, error bars indicate SEs and different letters indicate significant differences ($P < 0.05$): *indicates significant differences at $P < 0.05$, **indicates significant differences at $P < 0.01$. [Colour figure can be viewed at wileyonlinelibrary.com].

*LCD* expression. As shown in Figure 4(b), two 'TGACG' motifs, core sequences to which TGA3 binds, exist in the promoter region of *LCD* (Figure 4b). Subsequently, the interaction between TGA3 and the *LCD* promoter was confirmed by electrophoretic mobility shift assay (EMSA), in which fragment I (pLCD-1) covers the first 'TGACG' motif and fragment II (pLCD-2) covers the second one (Figure 4b). The recombinant TGA3 protein bound specifically to pLCD-1, and a competition assay using unlabeled pLCD-1 (ulpLCD-1) showed a proportionate decrease in the binding of TGA3 to pLCD-1, but unlabeled mutated pLCD-1 (umpLCD-1, in which the 'TGACG' motif was mutated to 'TCACG') did not compete with pLCD-1 for TGA3 binding (Figure 4c, left). Furthermore, TGA3 did not bind to mpLCD-1 because the core motif in the *LCD* promoter was mutated (Figure 4c, left). Additionally, a 6× His-tagged peptide was used as the protein control, and data showed that the peptide could not bind to the pLCD fragments. Similar results were also detected between TGA3, pLCD-2 and mpLCD-2 (Figure 4c, right). Thus, TGA3 bound specifically to pLCD-1 and pLCD-2 *in vitro*.

To further confirm that TGA3 can bind to the *LCD* promoter *in vivo*, chromatin immunoprecipitation (ChIP) combined with PCR was performed. The chromatin fractions from WT, with or without $Cr^{6+}$ stress, were isolated and used for ChIP analysis with antibodies against TGA3. The products precipitated by the anti-TGA3 antibody, as well as positive (Input) and negative (with pre-immune serum, NoAb) controls, were analyzed by real-time PCR using primers corresponding to pLCD-1 and pLCD-2. Both the

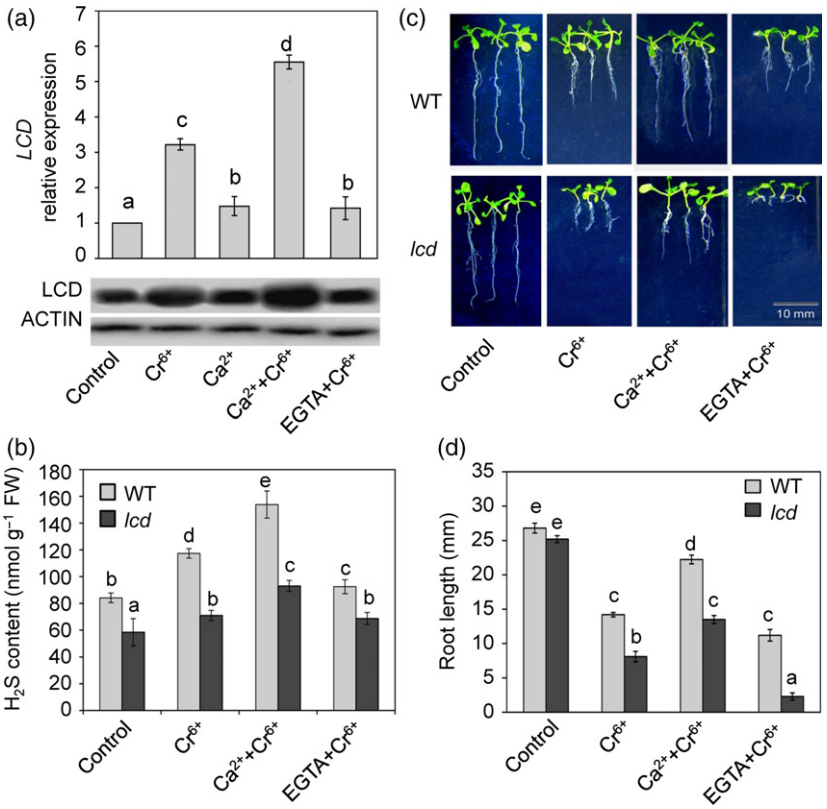


**Figure 3.** L-cysteine desulfhydrase (LCD)-mediated $H_2S$ generation was increased by $Ca^{2+}$ in the defense of Arabidopsis against $Cr^{6+}$ stress.
(a) The effects of $Ca^{2+}$ and EGTA on the $Cr^{6+}$-stress activated transcription and translation of *LCD*. The wild type (WT) was grown on 1/2 MS medium containing $Cr^{6+}$, $Ca^{2+}$, $Ca^{2+}$ + $Cr^{6+}$ or EGTA + $Cr^{6+}$. Two weeks later, the transcription and translation of *LCD* were detected by real-time quantitative RT-PCR and immunoblotting.
(b) The effects of $Ca^{2+}$ and EGTA on the $H_2S$ content in WT and *lcd* mutants with or without $Cr^{6+}$ stress. FW, fresh weight.
(c), (d) The effects of $Ca^{2+}$ and EGTA on root elongation in $Cr^{6+}$-stressed WT and *lcd* mutants.
The seeds of WT and *lcd* mutants were grown directly on 1/2 MS medium containing $Cr^{6+}$, $Ca^{2+}$ + $Cr^{6+}$ or EGTA + $Cr^{6+}$. Two weeks later, the endogenous $H_2S$ contents (b), the growth phenotypes (c) and the lengths of primary roots (d) were recorded from 20 seedlings. Data are means ± SE of three biological repeats, error bars indicate SEs and different letters indicate significant differences ($P < 0.05$). [Colour figure can be viewed at wileyonlinelibrary.com].

pLCD-1 and pLCD-2 fragments were pulled down by the anti-TGA3 antibody (Figure 4d), suggesting that TGA3 precisely bound to pLCD-1 and pLCD-2 *in vivo*. Moreover, this interaction seemed to be reinforced in $Cr^{6+}$-stressed plants (Figure 4d).

### $Ca^{2+}$/CaM2 interacted with TGA3 to enhance its binding to the *LCD* promoter, upregulating *LCD* expression during $Cr^{6+}$ stress

Interestingly, the pLCD-1 and pLCD-2 fragments were also precipitated by the anti-CaM2 antibody (Figure 4d), which indicated that CaM2 might interact with TGA3 to form a CaM2–TGA3–pLCD complex, and that the anti-CaM2 antibody might co-precipitate the pLCD fragments via TGA3 (Figure 4d). This conclusion was reinforced by the ChIP analysis of *tga3* and *cam2* loss-of-function mutants. The anti-TGA3 antibody did not precipitate the pLCD fragments in the *tga3* mutant, but did precipitate the pLCD fragments in the *cam2* mutant; however, the anti-CaM2 antibody cannot precipitate the pLCD fragments in either the *cam2* or *tga3* mutants (Figure 4d). Thus, TGA3 is an indispensable mediator in the formation of the CaM2–TGA3–pLCD complex.

The interaction between CaM2 and TGA3 *in vivo* was verified using co-immunoprecipitation (CoIP) analysis. Proteins extracted from WT, with or without $Cr^{6+}$ stress, were immunoprecipitated by anti-TGA3 and anti-CaM2 antibodies, respectively, and then the precipitates were analyzed with the appropriate antibody. Whether Arabidopsis seedlings were stressed by $Cr^{6+}$ or not, CaM2 and TGA3 bound to each other *in vivo* (Figure 5a). Because the $Cr^{6+}$ stress enhanced the transcription and translation of CaM2, but the TGA3 level was unchanged (Figure 4a), it can be speculated that the interaction of TGA3 and CaM2 was enhanced by $Cr^{6+}$ stress, mainly by upregulating the abundance of CaM2 protein.

To investigate the effects of $Ca^{2+}$/CaM2 on the combination of the TGA3 and *LCD* promoter, CaM2 or $Ca^{2+}$/CaM2 was added to the reaction system of EMSA to detect any interaction between TGA3 and pLCD-1 or pLCD-2. The binding affinity of TGA3 to pLCD-1 or pLCD-2 was enhanced by CaM2 and $Ca^{2+}$/CaM2. $Ca^{2+}$ strengthened the positive effects of CaM2 on the interaction between TGA3 and the *LCD* promoter (Figure 5b).

Additionally, the ability of CaM2 and TGA3 to regulate the activity of the *LCD* promoter was assayed *in vivo* by co-transforming tobacco leaves with the *TGA3* gene, the *CaM2* gene and the *LCD* promoter linked to a green fluorescent protein gene (p*LCD*-GFP). Notably, the reporter construct p*LCD*-GFP was maintained at the same concentration among the treatments and controls in each group of assays. TGA3 bound to the *LCD* promoter and enhanced its activity, as seen by the increased GFP-produced fluorescence (Figure 5c). Moreover, the co-expression of CaM2

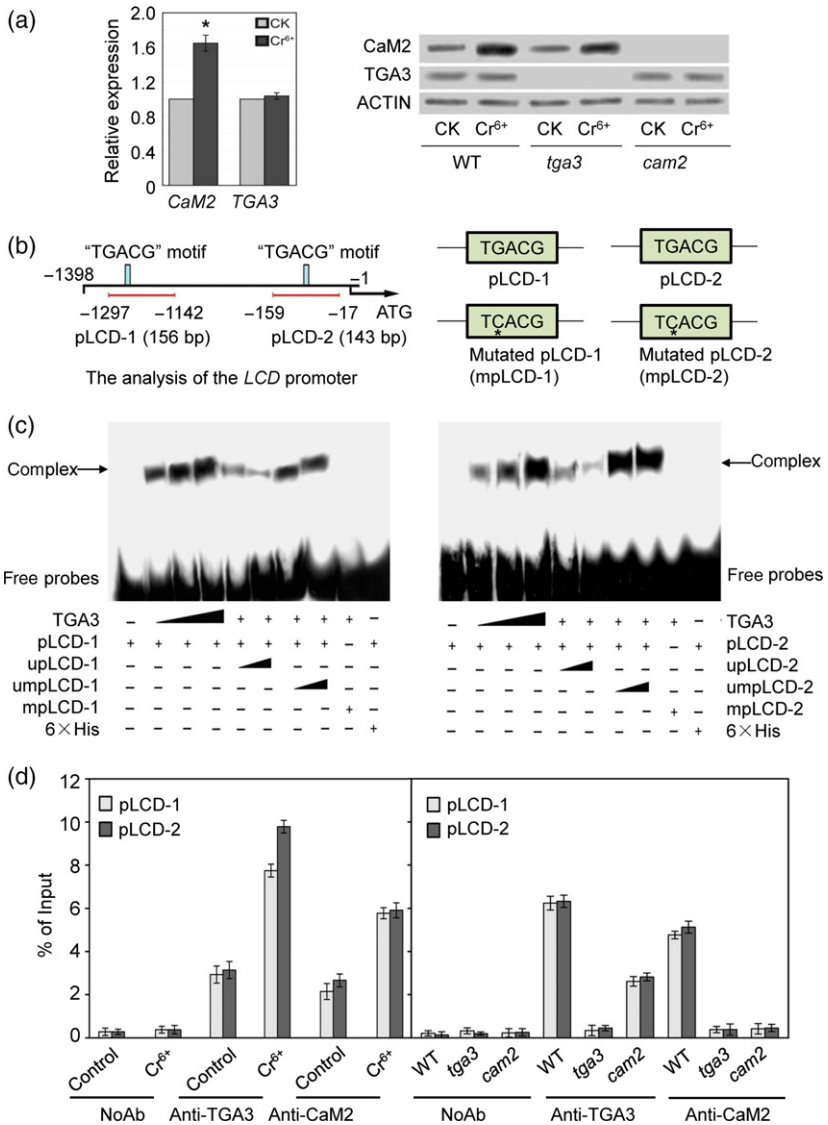


**Figure 4.** The calmodulin2 (CaM2)-associated transcription factor TGA3 specifically bound to the *LCD* promoter both *in vitro* and *in vivo*.
(a) The effect of $Cr^{6+}$ stress on the transcription and translation of *CaM2* and *TGA3*. The Arabidopsis wild type (WT), *tga3* and *cam2* mutants were grown on 1/2 MS medium with ($Cr^{6+}$) or without (CK) 180 μmol $L^{-1}$ $Cr^{6+}$. Two weeks later, *TGA3* and *CaM2* transcription and translation were detected by real-time quantitative RT-PCR and immunoblotting. Data are means ± SE of three biological repeats, error bars indicate SEs and *indicates significant differences at $P < 0.05$.
(b) An analysis of 'TGACG' motifs present in the *LCD* promoter. The vertical columns indicate the locations of 'TGACG' motifs in the *LCD* promoter. The lines (from −1297 to −1142 and −159 to −17) indicate the probes used in EMSA or the fragments, pLCD-1 and pLCD-2, analyzed in the chromatin immunoprecipitation (ChIP) assay. mpLCD-1 and mpLCD-2 represent pLCD-1 and pLCD-2, respectively, having 'TGACG' mutated to 'TCACG'. The asterisk represents the mutated nucleotide in the specific motif.
(c) Electrophoretic mobility shift assay of TGA3 binding to the 'TGACG' motifs in the *LCD* promoter. pLCD indicates the probes labeled with digoxigenin-11-dUTP, and mpLCD indicates the mutated probes labeled with digoxigenin-11-dUTP. upLCD indicates unlabeled probes and umpLCD indicates unlabeled mutated probes. upLCD and umpLCD were used to compete with pLCD for binding with the TGA3 recombinant protein. The labeled mutated probe mpLCD was used as a negative control; the 6× His (6× His-tagged peptide) was used as another protein control.
(d) ChIP analysis of CaM2–TGA3 binding to *LCD* promoter fragments. WT seedlings, with or without $Cr^{6+}$ stress, as well as the *tga3* and *cam2* loss-of-function mutants, were used for the ChIP assay. The chromatin fractions from these seedlings were immunoprecipitated by anti-TGA3 or anti-CaM2 antibodies. The non-immunoprecipitated sonicated chromatin was used as an input DNA control, and the chromatin precipitated with pre-immune serum (NoAb) was used as a negative control. The input DNA (diluted 50×) and the precipitated chromatin fragments were analyzed with real-time PCR using two primer sets amplifying the pLCD-1 and pLCD-2 fragments, as indicated in (b). The results are expressed as per cent of input. Three biological replications were performed and showed similar results. Each value is the mean ± SE of three independent experiments. [Colour figure can be viewed at wileyonlinelibrary.com].

obviously strengthened the activity of the TGA3-enhanced *LCD* promoter and exhibited a much stronger GFP fluorescence, while CaM2 alone could not alter the GFP fluorescence intensity (Figure 5c). These results were consistent with the EMSA observation that $Ca^{2+}$/CaM2 could enhance the binding affinity of TGA3 for the pLCD

fragments (Figure 5b). Thus, the observed increase in GFP intensity driven by the *LCD* promoter was caused by TGA3 or CaM2–TGA3. Additionally, CaM2 interacted with TGA3 and enhanced its ability to bind the *LCD* promoter; thereby strengthening the activation of the *LCD* transcription induced by TGA3.

### Both *cam2* and *tga3* loss-of-function mutants generated less $H_2S$ and were more sensitive to $Cr^{6+}$ stress

Under normal conditions, both transcription and translation (Figure 6a) of *LCD* were sharply reduced in *cam2* and *tga3* loss-of-function mutants, while the $H_2S$ contents in *cam2* and *tga3* were no different from that of the WT (Figure 6c). Interestingly, the abundance of LCD and the $H_2S$ content were significantly increased by $Cr^{6+}$ stress in the WT, but this $Cr^{6+}$ stress-associated activation did not occur in *cam2* and *tga3* mutants (Figure 6a–c). Furthermore, in the double mutants *tga3*/*lcd* and *cam2*/*lcd*, with or without $Cr^{6+}$ stress, both the LCD level and $H_2S$ content were significantly decreased (Figure 6a–c). These results were consistent with the functions of TGA3 and CaM2 in upregulating *LCD* expression and enhancing $H_2S$ emission.

We further detected the root growth of the *cam2*, *tga3*, *tga3*/*lcd* and *cam2*/*lcd* mutants. Like the *lcd* mutant, which is defective in producing $H_2S$, these mutants exhibited higher sensitivities to $Cr^{6+}$ stress, and root elongation in these mutants was suppressed more severely by $Cr^{6+}$ stress (Figure 6d). When these mutants were fumigated with exogenous $H_2S$, their $H_2S$ content significantly increased and the inhibition of root elongation caused by $Cr^{6+}$ stress was significantly relieved (Figure 6c, 6d),

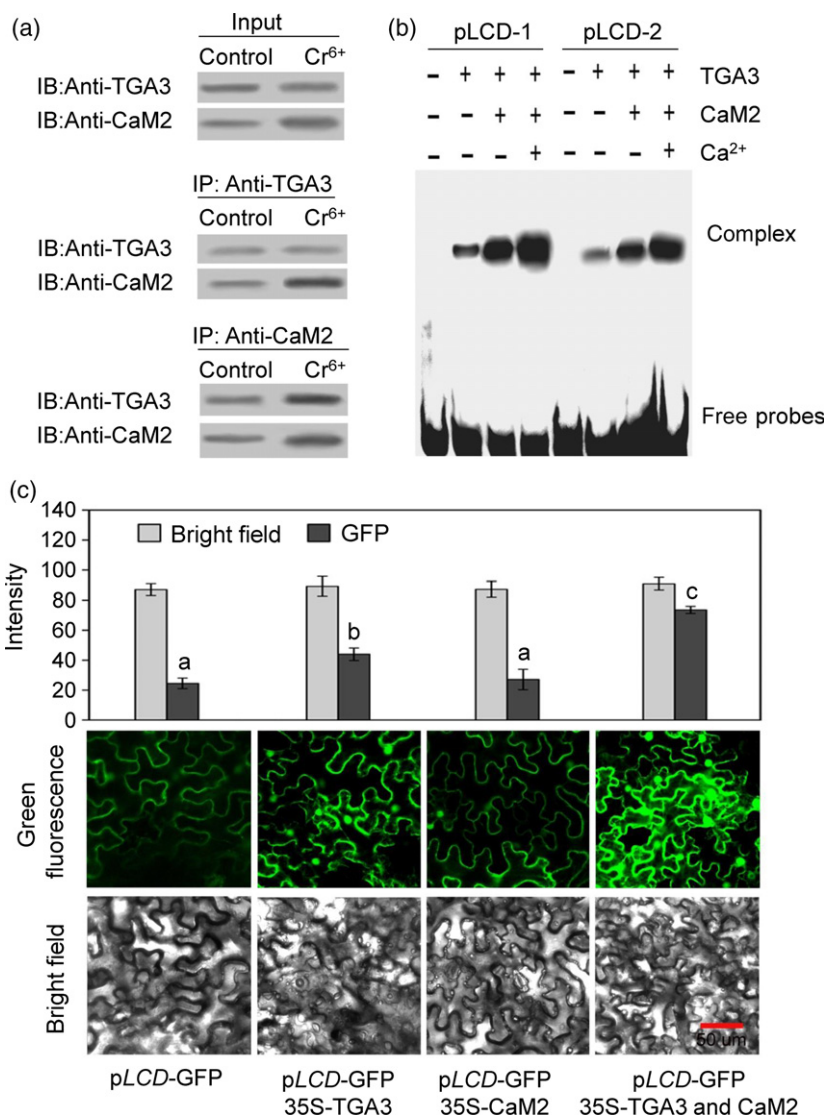


**Figure 5.** Calmodulin2 (CaM2) interacted with TGA3 and enhanced its binding ability to the *LCD* promoter.

(a) The combination of CaM2 and TGA3 in Arabidopsis with or without $Cr^{6+}$ stress. Protein extracted from the wild type (WT), with ($Cr^{6+}$) and without (CK) 180 μmol $L^{-1}$ $Cr^{6+}$ stress, was immunoprecipitated (IP) by anti-TGA3 or anti-CaM2 antibodies, respectively, and then the precipitates were immunoblotted (IB) with the appropriate antibodies.

(b) The effects of $Ca^{2+}$ and CaM2 on the binding activity of TGA3 to the *LCD* promoter. The TGA3-recombinant protein was incubated with labeled p*LCD* probes in the absence or presence of $Ca^{2+}$ and CaM2. The complexes were analyzed by electrophoretic mobility shift assay, and the experiments were repeated three times with similar results.

(c) The effects of CaM2 and TGA3 on the transcriptional activity of the *LCD* promoter. The effector constructs, CaMV 35S–TGA3 and CaMV 35S–CaM2, and the reporter construct p*LCD*–GFP, were transformed into tobacco leaves, and the green fluorescence intensities, which indicated the transcriptional activity of the *LCD* promoter, were observed using confocal laser scanning microscopy (Zeiss, LSM-880). Bars = 50 μm. The gray column indicates bright field intensities and the black column indicates green fluorescence intensities. The construct CaMV 35S–RFP was simultaneously transformed into the tobacco leaves as a control. Each value is the mean ± SE of three independent experiments, and different letters indicate significant differences ($P < 0.05$). [Colour figure can be viewed at wileyonlinelibrary.com].

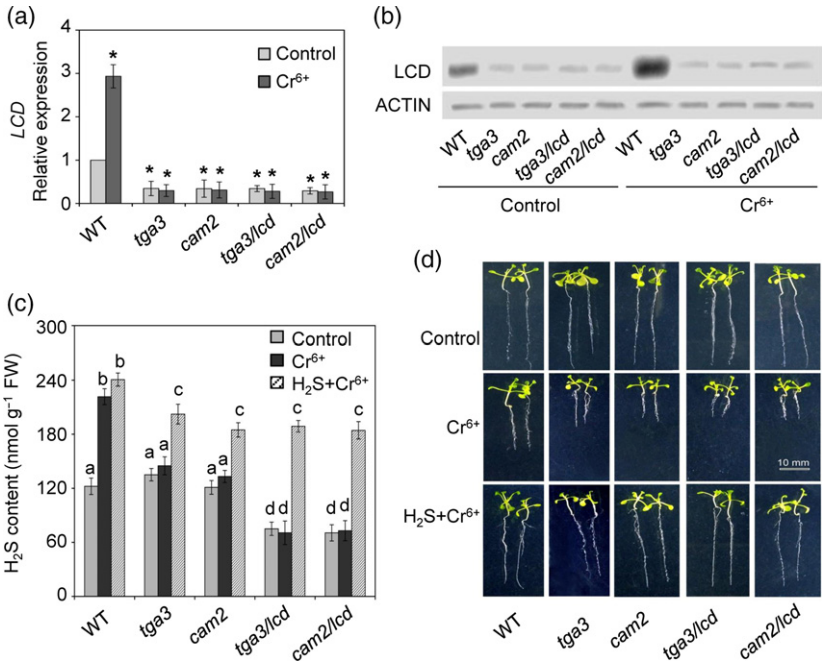


**Figure 6.** TGA3 and calmodulin2 (CaM2) are important in L-cysteine desulfhydrase (LCD) expression and $H_2S$ generation during defense of Arabidopsis against $Cr^{6+}$ stress.
(a), (b) The transcriptional and translational levels of *LCD* in *tga3*, *cam2*, *tga3/lcd* and *cam2/lcd* mutants with or without $Cr^{6+}$ stress.
(c) Effects of exogenous $H_2S$ fumigation on the $H_2S$ content in $Cr^{6+}$-stressed *tga3*, *cam2*, *tga3/lcd* and *cam2/lcd* mutants.
(d) Effects of exogenous $H_2S$ fumigation on the root elongation of wild type (WT), *tga3*, *cam2*, *tga3/lcd* and *cam2/lcd* mutants during $Cr^{6+}$ stress.
The seeds of WT, *tga3*, *cam2*, *tga3/lcd* and *cam2/lcd* Arabidopsis mutants were grown directly on 1/2 MS medium or 1/2 MS medium containing 180 μmol $L^{-1}$ $Cr^{6+}$. After growing for 2 weeks, the *LCD* transcriptional (a) and translational (b) levels, the $H_2S$ contents (c) and the growth phenotypes (d) were recorded from 20 seedlings. Data are means ± SE of three biological repeats, and error bars indicate the SE. *Significant differences at $P < 0.05$; different letters indicate significant differences ($P < 0.05$). [Colour figure can be viewed at wileyonlinelibrary.com].

supporting the conclusion that CaM2 and its binding transcription factor TGA3 acted upstream of *LCD* expression and $H_2S$ emission during defense against $Cr^{6+}$ stress in Arabidopsis.

## DISCUSSION

$H_2S$ is a versatile gasotransmitter, and different concentrations of $H_2S$ act differently in plants. Physiological levels of $H_2S$ mediate numerous positive functions, but a high level of $H_2S$ can be cytotoxic (Wang, 2012). Thus, to benefit from $H_2S$, it must be maintained at the appropriate level. Correspondingly, there must be some stress-targeted and stress-induced signals in plants to directly or indirectly modulate the $H_2S$ level, ensuring that the endogenous $H_2S$ emission is activated and that $H_2S$ remains at its physiological concentration. Under these conditions $H_2S$ acts as a transmitter that mediates the appropriate cellular responses in plants.

### The transcription factor TGA3 activated *LCD* expression and $H_2S$ emission in Arabidopsis under $Cr^{6+}$ stress by integrating into CaM2-mediated $Ca^{2+}$ signaling

A regulatory mechanism for endogenous $H_2S$ generation in $Cr^{6+}$-stressed seedlings was proposed based on this study, which indicated that $Ca^{2+}$/CaM2-mediated TGA3 functioned as a switch regulating *LCD* expression and modulating $H_2S$ generation during the response of Arabidopsis to $Cr^{6+}$ stress. As shown in Figure 7, $Cr^{6+}$ stress increased CaM2 expression, and then the CaM2-mediated $Ca^{2+}$ signal in Arabidopsis was received and the stress signal transmitted. After the loading of $Ca^{2+}$, CaM2 physically interacted with the bZIP transcription factor TGA3 and enhanced its binding affinity to the 'TGACG' *cis*-acting elements present in the *LCD* promoter, forming the $Ca^{2+}$/CaM2–TGA3–pLCD complex, which acted as a transcriptional activator to enhance *LCD* expression and then $H_2S$ production (Figure 7).

The assay for *trans*-activation ability in tobacco leaves illustrated that TGA3 enhanced p*LCD*-GFP fluorescence intensity, and co-expression of CaM2 strengthened the TGA3-induced increase in *LCD* promoter activity (Figure 5c). However, without TGA3, CaM2 alone had no *trans*-activation ability and could not alter the fluorescence intensity of p*LCD*-GFP (Figure 5c), suggesting that is TGA3 indispensable in $Ca^{2+}$/CaM2–TGA3–pLCD complex formation and *LCD* transcription. This was further supported by the ChIP analysis, in which the anti-CaM2 antibody could not precipitate the pLCD fragments in the *tga3* mutant, but the anti-TGA3 antibody could precipitate the pLCD fragments in the *cam2* mutant (Figure 4d).

Collectively, $Ca^{2+}$/CaM2 received and transmitted the $Cr^{6+}$ stress signal, and the CaM2-targeted TGA3 then acted as a pivotal regulator for activating *LCD* transcription and $H_2S$ emission. Subsequently, the activated endogenous $H_2S$ was utilized to induce appropriate cellular responses and fight against $Cr^{6+}$ stress (Figure 7). $H_2S$ acted as an gasotransmitter and then further induced cysteine accumulation, which increased the $Cr^{6+}$ stress tolerance of the Arabidopsis seedlings (Fang *et al.*, 2016). $Cr^{6+}$ stress-induced $H_2S$ acts as a gasotransmitter to upregulate the expression of the cysteine synthesis-related genes *SAT1*, *SAT5* and *OASTLa*, thus improving cysteine accumulation. The $H_2S$–

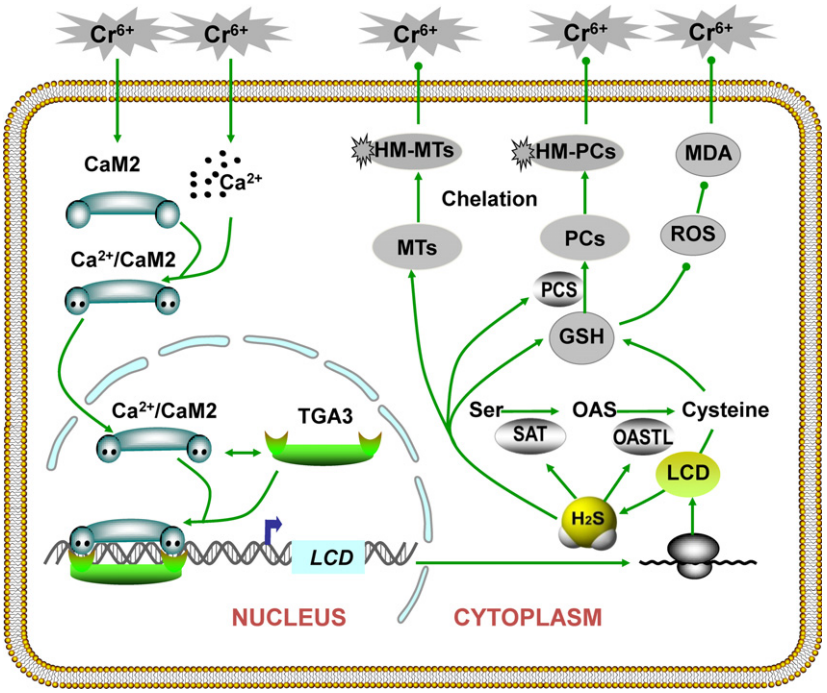


**Figure 7.** Model of how $Ca^{2+}$/calmodulin2 (CaM2) and TGA3 regulate *LCD* expression and $H_2S$ generation during defense against $Cr^{6+}$ stress in Arabidopsis.
Arrows indicate enhanced expression levels, and hyphens indicate suppressed expression levels. Ca, calcium; CaM, calmodulin; Cr, chromium; GSH, glutathione; $H_2S$, hydrogen sulfide; HMs, heavy metals; LCD, L-cysteine desulfhydrase; MT, metallothionein; OASTL, *O*-acetyl-L-serine (thiol) lyase; PC, phytochelatin; PCS, phytochelatin synthase; ROS, reactive oxygen species; SAT, serine acetyltransferase; Ser, serine; TGA, 'TGACG'-binding factor. [Colour figure can be viewed at wileyonlinelibrary.com].

cysteine signaling then participated in physiological processes that mediated metal detoxification, activating generation of the antioxidant GSH to relieve the $Cr^{6+}$ stress-associated oxidative damage and promoting the accumulation of HM chelators to chelate $Cr^{6+}$ (Figure 7) (Fang *et al.*, 2016).

Interestingly, Yang *et al.* reported that the activity of cystathionine γ-lyase (CSE), an important enzyme responsible for physiological generation of $H_2S$ in animals, could be activated by the $Ca^{2+}$/CaM pathway (Yang *et al.*, 2008). This was the first study to propose a correlation between $Ca^{2+}$ signaling and $H_2S$ production. In the current study, we propose a specific mechanism for enhancement of endogenous $H_2S$ generation by $Ca^{2+}$/CaM2, suggesting that $Ca^{2+}$/CaM2-enhanced *LCD* expression via TGA3-mediated transcriptional regulation.

### The interplay between $Ca^{2+}$, CaM2 and its target TGA3 increased the flexibility of transcriptional regulation of *LCD*

In this study, $Cr^{6+}$ stress did not change TGA3 expression, but increased the transcriptional and translational levels of CaM2 (Figure 4a), and correspondingly enhanced the interactions of CaM2 with its target protein TGA3 (Figure 5a). The EMSA analysis indicated that TGA3 bound specifically to the *LCD* promoter (Figure 4c) and that $Ca^{2+}$/CaM2 strengthened this combination (Figure 5b). Moreover, in $Cr^{6+}$-stressed seedlings, more *LCD* promoter fragments were precipitated by both anti-TGA3 and anti-CaM2 antibodies (Figure 4d, left). This suggested that $Cr^{6+}$ stress induced more stable $Ca^{2+}$/CaM2–TGA3–p*LCD* complexes to enhance *LCD* expression.

CaM, a small acidic protein that contains four EF hands for $Ca^{2+}$-binding, is the best characterized $Ca^{2+}$ sensor. Although CaM has no enzymatic activity of its own, it can interact with proteins and regulate their functions to transmit signals (Iqbal *et al.*, 2002). CaM responds to the elevation of cytosolic $Ca^{2+}$. Binding to $Ca^{2+}$ induces a conformational change in CaM and regulates its interactions with target proteins. Thus, $Ca^{2+}$/CaM-mediated signaling pathways are integrated into the plant's physiological responses to external stimuli (Kim *et al.*, 2009). The intracellular $Ca^{2+}$ level can be increased by $Cr^{6+}$ stress (Fang *et al.*, 2014). As shown in Figure 5(b), $Ca^{2+}$ enhanced the binding of CaM2 with TGA3 *in vitro*, and thus more $Ca^{2+}$/CaM2–TGA3–pLCD complexes were formed (Figure 5b), suggesting that CaM2 interacted with TGA3 in, at least partially, a $Ca^{2+}$-dependent manner. Conversely, CaM-targeted proteins or peptides can enhance the ability of CaM to bind $Ca^{2+}$ (Johnson *et al.*, 1996), and the enhancing effects of different target proteins on the $Ca^{2+}$–CaM combination are not identical (Zielinski, 1998). Accordingly, it is more appropriate to regard CaM2 as a tunable molecular modulator, rather than a simple on and off switch to initiate and transmit the $Ca^{2+}$ signal during $Cr^{6+}$ stress, activating *LCD* expression. $Ca^{2+}$ enhanced the combined effect of CaM2 and TGA3, while TGA3 may in turn modify the ability of CaM2 to bind to $Ca^{2+}$ through feedback loops; thus the CaM2-mediated cellular response can be modulated with more flexibility, not just on and off.

The sophisticated interplay between $Ca^{2+}$, CaM and the target proteins gives $Ca^{2+}$ signaling in plants a high level of complexity and flexibility when responding to stresses.

### Complicated interactions between the gasotransmitter $H_2S$ and $Ca^{2+}$ signaling during plant responses to environmental stimuli

Based on our model, we can interpret some previously reported phenomena. In our previous study, $Cr^{6+}$ stress caused a rapid increase in intracellular $Ca^{2+}$, and exogenous $Ca^{2+}$ strengthened $H_2S$ production induced by $Cr^{6+}$ stress in *Setaria italic* (Fang *et al.*, 2014). Coincidentally, Li *et al.* (2012) reported that $Ca^{2+}$ and CaM induced endogenous accumulation of $H_2S$, which increased thermotolerance in tobacco suspension cultured cells. Thus, $Ca^{2+}$ signaling, one of the earliest events in response to numerous stimuli, was activated to transmit the stress signal and finally induce the appropriate protective responses. Importantly, the modulation of $H_2S$ emission might be a critical step in $Ca^{2+}$/CaM-mediated stress defenses.

However, some studies found that $H_2S$ regulates $Ca^{2+}$ signaling to mediate cellular biological functions in plants. Li *et al.* (2012) reported that pre-treatment with NaHS promoted the entry of $Ca^{2+}$ into tobacco suspension cultured cells to increase heat tolerance (Li *et al.*, 2012). $H_2S$ can also regulate the expression of the $Ca^{2+}$ transporter, to close stomata in response to drought stress (Jin *et al.*, 2013). $H_2S$ can regulate some $Ca^{2+}$ sensors and interact with $Ca^{2+}$ signaling to enhance $Cr^{6+}$ tolerance in *S. italic* (Fang *et al.*, 2014). Thus, during the responses of plants to environmental stimuli, $Ca^{2+}$ signaling and $H_2S$ have complicated connections not a simple linear relationship. The $Ca^{2+}$ signal results from environmental stimuli and has a key role in modulating $H_2S$ functions that initiate some defense responses in plants. Conversely, $H_2S$ regulated $Ca^{2+}$ transporters and $Ca^{2+}$ sensors to further tune signaling transduction and complete the cycle. Thus, the interaction between $Ca^{2+}$ signaling and the gasotransmitter $H_2S$ appears to be more intricate than previously thought, and this topic demands more research.

Here, the $H_2S$ content was no different in the $Cr^{6+}$ and EGTA plus $Cr^{6+}$ treated *lcd* mutant (Figure 3b), but the EGTA plus $Cr^{6+}$ combined treatment had a more dramatic root phenotype and root elongation in *lcd* mutants was significantly suppressed (Figuer 3c, d). Thus, $Ca^{2+}$ signaling could also regulate root development in an *LCD*-independent manner, and in the EGTA-treated *lcd* mutant the $H_2S$ content decreased and the $Ca^{2+}$ signal was downregulated by EGTA; therefore, the effect of $Cr^{6+}$ toxicity on root growth was significantly increased (Figure 3c, d).

Additionally, the transcriptional regulation of *LCD* may be a key step in the $Ca^{2+}$ signaling-associated increase in $H_2S$ production; however, this is not the only pathway, because the activation effect of $Ca^{2+}$ on $H_2S$ emission was decreased, but not completely destroyed, in the $Cr^{6+}$-stressed *lcd* mutant (Figure 3b). This indicated that there were other $H_2S$-producing enzymes activated by $Ca^{2+}$ signaling during the response of Arabidopsis to $Cr^{6+}$ stress.

The endogenous $H_2S$ content in $Cr^{6+}$-stressed *cam2* and *tga3* was much lower than that in the WT (Figure 6c), which made the mutants more sensitive to $Cr^{6+}$ stress (Figure 6d). Thus, the defect in CaM2 or TGA3 decreased endogenous $H_2S$ generation, reducing the ability of the mutants to defend against $Cr^{6+}$ stress. Interestingly, during normal condition, *LCD* transcription and translation decreased obviously in *cam2* and *tga3* (Figure 6a, b), but the $H_2S$ content showed no obvious difference between the WT and mutants (Figure. 6c). This suggested that there may be other signals or other $H_2S$-producing enzymes than LCD in *cam2* and *tga3* to supplement $H_2S$ emission. In other words, there are precise regulatory pathways for maintaining a basic level of $H_2S$ in these mutants. However, although *cam2* and *tga3* have supplementary pathways for $H_2S$ content, $Cr^{6+}$ stress still could not increase the $H_2S$ content to a higher level (Figure 6c), suggesting that the $Ca^{2+}$/CaM2-TGA3-mediated regulation of *LCD* transcription was dominant in activating $H_2S$ emissions during defense against $Cr^{6+}$ stress in Arabidopsis. This was supported the higher sensitivities to $Cr^{6+}$ stress of *cam2* and *tga3* (Figure 6d). The root lengths of the double mutants *tga3*/*lcd* and *cam2*/*lcd* were much shorter than in the WT during $Cr^{6+}$ stress, indicating that CaM2 and TGA3 acted upstream of *LCD* expression. These results highlight the importance of CaM2-mediated $Ca^{2+}$ signaling in regulating endogenous $H_2S$ emission during the response of Arabidopsis to $Cr^{6+}$ stress.

$H_2S$ functions as a gasotransmitter in plant defenses against numerous stresses, and the appropriate level of $H_2S$ can reduce the accumulation of HMs in millet (Tian *et al.*, 2017). Our results indicated a regulatory pathway for endogenous $H_2S$ emission in the responses of Arabidopsis to $Cr^{6+}$ stress. The results also emphasized the important role of CaM2-targeted TGA3 in tuning *LCD* expression, and hence $H_2S$ production, suggesting that manipulation of the endogenous $H_2S$ level through genetic engineering may assist agricultural production on soil contaminated with HMs. Recently, the $H_2S$ target proteins, as well as the interactions between $H_2S$ and other signals in the $H_2S$ regulatory network, have attracted attention. The focus is currently on the proteins' S-sulfhydration and polysulfide reactions mediated by $H_2S$, which may require the transition of intermediate links and the contribution of other signals.

## EXPERIMENTAL PROCEDURES

### Plant materials

Seeds of *A. thaliana* WT (Columbia, Col-0), the *LCD* T-DNA insertion mutant *lcd* (SALK_082099), the *TGA3* T-DNA insertion

mutant *tga3* (SALK_086928) and the *CaM2* T-DNA insertion mutant *cam2* (SALK_089283) were employed in this research. The seeds of *lcd* were obtained from the Arabidopsis Biological Resource Center (http://www.arabidopsis.org/abrc/). The *tga3* mutant was kindly provided by Jiawei Wang (Institute of Plant Physiology and Ecology, Shanghai Institutes for Biological Sciences, Chinese Academy of Sciences, China). The *cam2* mutant was kindly provided by Weicai Yang (Institute of Genetics and Developmental Biology, Chinese Academy of Sciences, China). After stratification at 4°C, seeds were sterilized in 75% ethanol for 50 sec and 6% sodium hypochlorite for 8 min under sterile conditions. After washing with sterile water three times, seeds were grown on 1/2 MS medium with or without additional treatments under a 16-h/8-h (light/dark) photoperiod, with light illumination at 160 E $m^{-2}$ $sec^{-1}$, at 23°C, with 60% relative humidity.

For $Cr^{6+}$ stress, a sterile $K_2Cr_2O_7$ solution was added directly to the 1/2 MS medium. For $Ca^{2+}$ treatment, a sterile $CaCl_2$ solution was added to the 1/2 MS medium and the final concentration of $Ca^{2+}$ was 20 mmol $L^{-1}$ (the data for selecting the effective concentration of $Ca^{2+}$ are shown in the Figure S1 in the Supporting Information). For $Ca^{2+}$ deprivation, the 1/2 MS medium was coated with a sterile solution of 5 mmol $L^{-1}$ EGTA. For the $H_2S$ treatment, the materials were kept in Petri dishes placed in a sealed glass container and then fumigated with 50 μmol $L^{-1}$ $H_2S$, which was released from NaHS, a widely recognized $H_2S$ donor, and all of the manipulations were performed as described previously (Fang *et al.*, 2014).

### RNA extraction and real-time quantitative RT-PCR

Two-week-old seedlings were collected for total RNA extraction with RNA isolation TRIzol® Reagent (Invitrogen, http://www.invitrogen.com/), according to the manufacturer's instructions. The cDNAs used for real-time quantitative RT-PCR (qRT-PCR) were synthesized using a reverse transcription system kit (TaKaRa, http://www.takara-bio.com/) and oligo(dT) primers. All of the primer pairs used for qRT-PCR were checked for amplification specificity and are listed in Table S1. *Ubiquitin4* (*UBQ4*, *At5g20620*) was used as the internal control. A Bio-Rad Real-Time System (CFX96TM C1000 Thermal Cycler, http://www.bio-rad.com/) was used to perform qRT-PCR.

### Determination of the $H_2S$ production rate and $H_2S$ content

Total protein extracts were collected from 2-week-old seedlings, then L-cysteine was added as a substrate in the extracts to determine the $H_2S$ production rate using a previously published protocol (Jin *et al.*, 2013). The endogenous $H_2S$ content was detected using a novel polarographic $H_2S$ sensor (WPI, TBR4100, https://www.wpiinc.com/), and all of the manipulations were performed according to a previous publication (Riemenschneider, 2006).

### Production of recombinant proteins TGA3 and CaM2

The cDNAs encoding TGA3 (At1g22070) and CaM2 (At2g41110.1) were cloned into the 6× His-tagged vector pET28a. After checking their accuracy, the plasmids were independently transformed into *Escherichia coli* BL21, and 1 mmol $L^{-1}$ isopropyl β-D-thiogalactopyranoside (IPTG) was used to induce TGA3 expression at 16°C or 0.5 mmol $L^{-1}$ IPTG to induce CaM2 expression at 28°C. The recombinant proteins were purified with the $Ni^{2+}$-chelating column according to the manufacturer's instructions. The purified proteins were used for *in vitro* experiments and antibody preparation.

### Electrophoretic mobility shift assay

The EMSA was executed according to a previously published method (Liu *et al.*, 2012). The recombinant 6× His-TGA3 and 6× His-CaM2 proteins purified from *Escherichia coli* BL21 were used for EMSA. For probes, the promoter fragments (pLCD-1 and pLCD-2) and the site-specific mutated pLCD fragments (mpLCD-1 and mpLCD-2) were amplified and labeled with digoxigenin-11-dUTP (Roche, http://www.roche.com/) according to the manufacturer's instructions. The primers used for probe amplification are listed in Table S1.

The labeled probes and recombinant proteins were incubated in binding buffer [10 mM 2-amino-2-(hydroxymethyl)-1,3-propanediol (TRIS)-HCl (pH 8.0), 20 mM NaCl, 0.4 mM $MgCl_2$, 0.25 mM EDTA and 0.25 mM DTT] at 25°C for 30 min, with poly (dI-dC) as a non-specific competitor. Then, the samples were separated on a 5% polyacrylamide gel (19:1 acrylamide:bisacrylamide) and transferred onto a nylon filter membrane (Hybond-$N^+$, GE, http://www.gelifesciences.com/). After UV crosslinking, the membrane was blocked in blocking reagent for 2 h and incubated with the anti-digoxigenin-AP antibody for 1 h. The result was detected using a CDP-star-based detection kit (Roche).

### *Trans*-activation ability assay in tobacco leaves

This assay was performed as previously described (Liu *et al.*, 2012). To obtain the effector constructs, the cDNAs of *TGA3* (*At1g22070*) and *CaM2* (*At2g41110.1*) were amplified and fused to the pCAMBIA1302 vector downstream of the cauliflower mosaic virus (CaMV) 35S promoter at the *Bam*HI/*Hin*dIII sites and *Nco*I/*Pst*I sites, respectively. The primer pairs are listed in Table S1. For the reporter construct, the *GFP* gene was driven by the *LCD* promoter (−1 bp to −1398 bp), which was fused to the *Pst*I/*Kpn*I sites and replaced the CaMV 35S promoter in pCAMBIA1300. These constructs were mobilized into *Agrobacterium tumefaciens* strain GV3101 and infiltrated into young but fully expanded leaves of 7-week-old *Nicotiana benthamiana* plants using a needleless syringe. The concentration of the reporter construct p*LCD*-GFP should be identical among treatments and controls in each assay group. After infiltration, plants were kept in the dark for 12 h and then transferred to a 16-h/8-h (light/dark) photoperiod for 60 h. Subsequently, the GFP fluorescence was observed by confocal laser scanning microscopy (LSM-880, Zeiss, https://www.zeiss.com/). The experiments were repeated five times independently, with similar results.

### Chromatin immunoprecipitation assay

The ChIP assay was performed as previously described (Pei *et al.*, 2007; Mukhopadhyay *et al.*, 2008). WT seedlings, with or without $Cr^{6+}$ stress, as well as the *tga3* and *cam2* loss-of-function mutants, were used for the ChIP assay. Four-week-old seedlings were immersed in the crosslinking buffer, which contained 0.4 M sucrose, 10 mM TRIS-HCl (pH 8.0), 1 mM phenylmethanesulfonyl fluoride (PMSF), 5 mM β-mercaptoethanol and 1% formaldehyde, for a 10-min vacuum treatment, and glycine (0.125 M) was added to terminate the reaction with an additional 5-min vacuum treatment. Subsequently, the seedlings were ground rapidly in liquid nitrogen, and the resuspended chromatin was sonicated to fragments of 0.5–2.0 kb at 4°C. The sheared chromatin was incubated in ChIP dilution buffer [16.7 mM TRIS-HCl (pH 8.0), 167 mM NaCl, 1.2 mM EDTA, 1 mM PMSF and 1.1% Triton X-100]. After pre-combination with 20 μl of Protein G Agarose/Salmon Sperm DNA (16-201, Upstate, http://www.merck.cn/zh/index.html) for 1 h at 4°C with gentle rotation, the chromatin was recovered and incubated

with the appropriate antibodies overnight at 4°C. The pre-immune serum, instead of the antibody, was the negative control. Then, 40 μl of Protein G Agarose/Salmon Sperm DNA was added to the mixture for a further 2-h incubation at 4°C. Subsequently, the agarose beads were collected, and the immunoprecipitated chromatin was isolated by reversing crosslinking. The non-immunoprecipitated sonicated chromatin was reverse crosslinked and used as an input DNA control. Both immunoprecipitated DNA and input DNA were analyzed by PCR.

The polyclonal anti-TGA3 antibody (10 000×) and anti-CaM2 antibody (20 000×), made by the Biology Institute of Shanxi (http://www.sxsws.com/), were used to immunoprecipitate TGA3 and CaM2, which in turn pulled down bound DNA fragments.

The experiment was repeated independently with three biological replicates, with similar results.

### Co-immunoprecipitation assay

The CoIP assays were performed as previously described (Shang *et al.*, 2010). Approximately 0.6 mg of 4-week-old Arabidopsis seedlings was ground in liquid nitrogen and then resuspended in 1 ml of extraction buffer containing 50 mM TRIS-HCl (pH 7.4), 150 mM NaCl, 1 mM EDTA, 0.1% Triton X-100, 10% glycerol, 1 mM PMSF and 1× protease inhibitor cocktail. The protein extract was then collected by centrifugation at 12 000***g*** for 5 min at 4°C. After pre-incubation with protein G agarose beads, the protein extract was incubated with the anti-TGA3 (10 000×) or anti-CaM2 antibody (20 000×) at 4°C overnight with gentle rotation. Subsequently, the protein G agarose beads were added. After incubation at 4°C with gentle rotation for 3 h, the beads were collected and washed three times with extraction buffer and resuspended. The immunoprecipitates were separated on a 12% SDS-PAGE and analyzed by immunoblotting with anti-TGA3 (10 000×) or anti-CaM2 antibody (20 000×).

## ACKNOWLEDGEMENTS

We are grateful to Dr Jiawei Wang for providing the *tga3* mutant seeds and Dr Weicai Yang for providing the *cam2* mutant seeds. The laboratory group of Jixian Zhai was supported by the Thousand Talents Program for Young Scholars and Southern University of Science and Technology. This work was supported by the National Natural Science Foundation of China (award 31671605 and 31372085 to Yanxi Pei; award 31672140 to Zhuping Jin). We sincerely appreciate Dr Juanjuan Wang (Scientific Instrument Center of Shanxi University) for her scientific inputs into our research.

## CONFLICTS OF INTEREST

The authors declare that there are no conflicts of interest.

## SUPPORTING INFORMATION

Additional Supporting Information may be found in the online version of this article.

**Figure S1.** The effects of $Ca^{2+}$ on the root growth and $H_2S$ production rate in $Cr^{6+}$ stressed Arabidopsis.

**Table S1.** Primers used in this study.

## REFERENCES

**Alvarez, C., Calo, L., Romero, L.C., García, I. and Gotor, C.** (2009) An O-acetylserine(thiol)lyase homolog with L-cysteine desulfhydrase activity regulates cysteine homeostasis in *Arabidopsis*. *Plant Physiol.* **152**, 656–669.

**Chen, J., Wang, W.H., Wu, F.H., He, E.M., Liu, X., Shangguan, Z.P. and Zheng, H.L.** (2015) Hydrogen sulfide enhances salt tolerance through nitric oxide-mediated maintenance of ion homeostasis in barley seedling roots. *Sci. Rep.* **5**. Available at: https://doi.org/10.1038/srep12516.

**Christou, A., Manganaris, G.A., Papadopoulos, I. and Fotopoulos, V.** (2013) Hydrogen sulfide induces systemic tolerance to salinity and non-ionic osmotic stress in strawberry plants through modification of reactive species biosynthesis and transcriptional regulation of multiple defence pathways. *J. Exp. Bot.* **64**, 1953–1966.

**Doherty, C.J., Buskirk, H.A.V., Myers, S.J. and Thomashow, M.F.** (2009) Roles for *Arabidopsis* CAMTA transcription factors in cold-regulated gene expression and freezing tolerance. *Plant Cell*, **21**, 972–984.

**Fang, H., Tao, J., Liu, Z., Zhang, L., Jin, Z. and Pei, Y.** (2014) Hydrogen sulfide interacts with calcium signaling to enhance the chromium tolerance in Setaria italica. *Cell Calcium*, **56**, 472–481.

**Fang, H.H., Liu, Z.Q., Jin, Z.P., Zhang, L.P., Liu, D.M. and Pei, Y.X.** (2016) An emphasis of hydrogen sulfide-cysteine cycle on enhancing the tolerance to chromium stress in *Arabidopsis*. *Environ. Pollut.* **213**, 870–877.

**Galon, Y., Finkler, A. and Fromm, H.** (2010) Calcium-regulated transcription in plants. *Molecular Plant*, **3**, 653–669.

**Harrington, H.M. and Smith, I.K.** (1980) Cysteine metabolism in cultured tobacco cells. *Plant Physiol.* **65**, 151–155.

**Heeg, C.** (2008) Analysis of the *Arabidopsis* O-acetylserine(thiol)lyase gene family demonstrates compartment-specific differences in the regulation of cysteine synthesis. *Plant Cell*, **20**, 168–185.

**Hetherington, A.M. and Brownlee, C.** (2004) The generation of $Ca^{2+}$ signals in plants. *Annu. Rev. Plant Biol.* **55**, 401–427.

**Honda, K.** (2015) 8-Mercapto-Cyclic GMP mediates hydrogen sulfide-induced stomatal closure in *Arabidopsis*. *Plant Cell Physiol.* **56**, 1481–1489.

**Iqbal, M., Galibert, J., Wasim, S.M., Hernandez, E., Bocaranda, P. and Leotin, J.** (2002) Calmodulin in action: diversity in target recognition and activation mechanisms. *Cell*, **108**, 739–742(734).

**Jakoby, M., Weisshaar, B., Dröge-Laser, W., Vicente-Carbajosa, J., Tiedemann, J., Kroj, T. and Parcy, F.** (2002) bZIP transcription factors in *Arabidopsis*. *Trends Plant Sci.* **7**, 106–111.

**Jia, H., Hu, Y., Fan, T. and Li, J.** (2014) Hydrogen sulfide modulates actin-dependent auxin transport via regulating ABPs results in changing of root development in *Arabidopsis*. *Sci. Rep.* **5**. Available at: https://doi.org/10.1038/srep08251.

**Jin, Z.P. and Pei, Y.X.** (2015) Physiological implications of hydrogen sulfide in plants: pleasant exploration behind its unpleasant odour. *Oxid Med Cell Longev*. Available at: http://dx.doi.org/10.1155/2015/397502.

**Jin, Z.P., Xue, S.W., Luo, Y.N., Tian, B.H., Fang, H.H., Hua, L. and Pei, Y.X.** (2013) Hydrogen sulfide interacting with abscisic acid in stomatal regulation responses to drought stress in *Arabidopsis*. *Plant Physiol. Biochem.* **62**, 41–46.

**Johnson, J.D., Snyder, C., Walsh, M. and Flynn, M.** (1996) Effects of myosin light chain kinase and peptides on $Ca^{2+}$ exchange with the N- and C-terminal $Ca^{2+}$ binding sites of calmodulin. *J. Biol. Chem.* **271**, 761–767.

**Kim, M.C., Chung, W.S., Yun, D. and Cho, M.J.** (2009) Calcium and calmodulin-mediated regulation of gene expression in plants. *Molecular Plant*, **2**, 13–21.

**Kudla, J., Batistič, O. and Hashimoto, K.** (2010) Calcium signals: the lead currency of plant information processing. *Plant Cell*, **22**, 541–563.

**Li, Z.G.** (2013) Hydrogen sulfide: A multifunctional gaseous molecule in plants. *Russ. J. Plant Physiol.* **60**, 733–740.

**Li, Z.G., Gong, M., Xie, H., Yang, L. and Li, J.** (2012) Hydrogen sulfide donor sodium hydrosulfide-induced heat tolerance in tobacco (*Nicotiana tabacum* L.) suspension cultured cells and involvement of $Ca^{2+}$ and calmodulin. *Plant Sci.* **185**, 185–189.

**Liu, Z.Q., Yan, L., Wu, Z., Mei, C., Lu, K., Yu, Y.T., Liang, S., Zhang, X.F., Wang, X.F. and Zhang, D.P.** (2012) Cooperation of three WRKY-domain transcription factors WRKY18, WRKY40, and WRKY60 in repressing two ABA-responsive genes ABI4 and ABI5 in *Arabidopsis*. *J. Exp. Bot.* **63**, 6371–6392.

**Miao, Z.H. and Lam, E.** (1995) Targeted disruption of the TGA3 locus in *Arabidopsis thaliana*. *Plant J.* **7**, 359–365.

**Miao, Z.H., Liu, X. and Lam, E.** (1994) TGA3 is a distinct member of the TGA family of bZIP transcription factors in *Arabidopsis thaliana*. *Plant Mol. Biol.* **25**, 1–11.

**Mukhopadhyay, A., Deplancke, B., Walhout, A.J. and Tissenbaum, H.A.** (2008) Chromatin immunoprecipitation (ChIP) coupled to detection by quantitative real-time PCR to study transcription factor binding to DNA in *Caenorhabditis elegans*. *Nature Protocol*, **3**, 698–709.

**Pagnussat, G.C., Lanteri, M.L., Lombardo, M.C. and Lamattina, L.** (2004) Nitric oxide mediates the indole acetic acid induction activation of a mitogen-activated protein kinase cascade involved in adventitious root development. *Plant Physiol.* **135**, 279–286.

**Papanatsiou, M., Scuffi, D., Blatt, M.R. and García-Mata, C.** (2015) Hydrogen sulphide regulates inward-rectifying $K^+$ channels in conjunction with stomatal closure. *Plant Physiol.* **168**, 29–35.

**Papenbrock, J., Riemenschneider, A., Kamp, A., Schulz-Vogt, H.N. and Schmidt, A.** (2007) Characterization of cysteine-degrading and $H_2S$-releasing enzymes of higher plants - from the field to the test tube and back. *Plant Biology*, **9**, 582–588.

**Park, C.Y., Lee, J.H., Yoo, J.H., Moon, B.C., Kang, Y.H., Lee, S.M., Kim, H.S., Kang, K.Y., Chung, W.S. and Lim, C.O.** (2005) WRKY group IId transcription factors interact with calmodulin. *FEBS Lett.* **579**, 1545–1550.

**Pei, Y.X., Niu, L.F., Lu, F.L., Liu, C.Y., Zhai, J.X., Kong, X.F. and Cao, X.F.** (2007) Mutations in the type II protein Arginine Methyltransferase AtPRMT5 result in pleiotropic developmental defects in *Arabidopsis*. *Plant Physiol.* **144**, 1913–1923.

**Peiter, E.** (2011) The plant vacuole: Emitter and receiver of calcium signals. *Cell Calcium*, **50**, 120–128.

**Rennenberg, H., Arabatzis, N. and Grundel, I.** (1987) Cysteine desulphydrase activity in higher plants: Evidence for the action of L- and D-cysteine specific enzymes. *Phytochemistry*, **26**, 1583–1589.

**Riemenschneider, A.** (2006) *Isolation and characterization of cysteine-degrading and H2S-releasing proteins in higher plants*. Hannover: University of Hannover.

**Romero, L.C., Garcia, I. and Gotor, C.** (2013) L-Cysteine Desulfhydrase 1 modulates the generation of the signaling molecule sulfide in plant cytosol. *Plant Signal Behav*, **8**. Available at: https://doi.org/10.4161/psb.24007.

**Sanders, D., Pelloux, J., Brownlee, C. and Harper, J.F.** (2002) Calcium at the crossroads of signaling. *Plant Cell*, **14**(Suppl), S401–417.

**Shang, Y., Yan, L., Liu, Z.Q., Cao, Z., Mei, C., Xin, Q., Wu, F.Q., Wang, X.F., Du, S.Y. and Jiang, T.** (2010) The Mg-Chelatase H subunit of *Arabidopsis* antagonizes a group of WRKY transcription repressors to relieve ABA-responsive genes of inhibition. *Plant Cell*, **22**, 1909–1935.

**Shanker, A.K., Cervantes, C., Loza-Tavera, H. and Avudainayagam, S.** (2005) Chromium toxicity in plants. *Environ. Int.* **31**, 739–753.

**Shi, H., Ye, T. and Chan, Z.** (2013) Exogenous application of hydrogen sulfide donor sodium hydrosulfide enhanced multiple abiotic stress tolerance in bermudagrass (*Cynodon dactylon* (L). Pers.). *Plant Physiol. Biochem.* **71**, 226–234.

**Shi, H., Ye, T. and Chan, Z.** (2014) Nitric oxide-activated hydrogen sulfide is essential for cadmium stress response in bermudagrass (*Cynodon dactylon* (L). Pers.). *Plant Physiol. Biochem.* **74**, 93–98.

**Szymanski, D.B. and Zielinski, R.E.** (1996) Calmodulin isoforms differentially enhance the binding of cauliflower nuclear proteins and recombinant TGA3 to a region derived from the *Arabidopsis Cam*-3 promoter. *Plant Cell*, **8**, 1069–1077.

**Tian, B.H., Zhang, Y.J., Jin, Z.P., Liu, Z.Q. and Pei, Y.X.** (2017) Role of hydrogen sulfide in the methyl jasmonate response to cadmium stress in *foxtail millet*. *Front Biosci.* **22**, 530–539.

**Wang, R.** (2002) Two's company, three's a crowd: can $H_2S$ be the third endogenous gaseous transmitter? *FASEB J.* **16**, 1792–1798.

**Wang, R.** (2012) Physiological implications of hydrogen sulfide: a whiff exploration that blossomed. *Physiol. Rev.* **92**, 791–896.

**Wang, L., Wan, R., Shi, Y. and Xue, S.** (2016) Hydrogen Sulfide activates S-type anion channel via OST1 and $Ca^{2+}$ modules. *Molecular Plant*, **9**, 489–491.

**Wei, B.G. and Yang, L.S.** (2010) A review of heavy metal contaminations in urban soils, urban road dusts and agricultural soils from China. *Microchem. J.* **94**, 99–107.

**Wilson, L.G., Bressan, R.A. and Filner, P.** (1978) Light-dependent emission of Hydrogen Sulfide from plants. *Plant Physiol.* **61**, 184–189.

**Yang, G., Wu, L., Jiang, B., Yang, W., Qi, J., Cao, K., Meng, Q., Mustafa, A.K., Mu, W. and Zhang, S.** (2008) $H_2S$ as a physiologic vasorelaxant: hypertension in mice with deletion of cystathionine $\gamma$-lyase. *Science*, **322**, 587–590.

**Zhang, H., Hu, L.Y., Hu, K.D., He, Y.D., Wang, S.H. and Luo, J.P.** (2009) Hydrogen Sulfide promotes wheat seed germination and alleviates oxidative damage against copper stress. *J. Integr. Plant Biol.* **50**, 1518–1529.

**Zhang, H., Hu, S.L., Zhang, Z.J., Hu, L.Y., Jiang, C.X., Wei, Z.J., Liu, J., Wang, H.L. and Jiang, S.T.** (2011) Hydrogen sulfide acts as a regulator of flower senescence in plants. *Postharvest Biol. Technol.* **60**, 251–257.

**Zielinski, R.E.** (1998) Calmodulin and Calmodulin-binding proteins in plants. *Annu. Rev. Plant Biol.* **49**, 697–725.